*IFSCC 2025 full paper (**IFSCC2025-1075**)*

CCN1: The Key to Sensitive Skin Aging Ecology — Ashwagandha as a Scientific Solution for Holistic Beauty and Wellness

Yanhong Liu[1], Zhiting Zhang[1], Lin Geng[1], Shuangyan Wang[1], Mingying Yu[1], Shaojie Gu[1], HuaJun Shi[1], JianFang Luo[1], Naisheng Jiang[2] ,Shaochun Cai[3] , Li Ye[4,5]*, Yue Zhang[6]*, Dongcui Li[1]*

[1] Research and Development, Hua An Tang Biotech Group Co., Ltd., Guangzhou, China; [2] Key Laboratory of Advanced Materials and Devices for Post-Moore Chips, Ministry of Education, School of Materials Science and Engineering, University of Science and Technology Beijing, Beijing, China；[3] Skin Lane (Guang Zhou) Biotech Co., Ltd., Guangzhou, China；[4] Dermatology Hospital, Southern Medical University, Guangzhou, Guangdong, China；[5] Hygiene Detection Center,School of Public Health, Southern Medical University(NMPA Key Laboratory for Safety Evaluation of Cosmetics, Guangdong Provincial Key Laboratory of Tropical Disease Research), Guangzhou, Guangdong, China；[6] Key Laboratory of Advanced Materials and Devices for Post-Moore Chips, Ministry of Education, School of Materials Science and Engineering, University of Science and Technology Beijing, Beijing, China.

---

1. Introduction

The term sensitive skin was first introduced by Bernstein in 1947 to describe adverse cutaneous reactions caused by soap cleansing [1]. In 2016, the International Forum for the Study of Itch (IFSI) provided an official definition, describing sensitive skin as a syndrome characterized by unpleasant sensations (stinging, burning, pain, pruritus, and tingling) in response to stimuli that do not typically provoke such reactions [2]. Sensitive skin is now recognized as a prevalent condition worldwide, affecting a significant proportion of the population across diverse geographic regions [3-5]. Reported prevalence ranges from 25.4% to 89.9% in Europe, ~50% in Australia, 22.3% to 50.9% in the Americas, and 40% to 55.98% in Asia, with a prevalence of 36.1% among Chinese women [6]. The rising incidence of sensitive skin is closely linked to increasing environmental pollution and psychosocial stress [2, 3, 5]. In response, clinical guidelines such as the Chinese Clinical Guidelines for the Diagnosis and Treatment of Sensitive Skin (2024 Edition) have been developed to support dermatological diagnosis and intervention. These guidelines emphasize that sensitive skin involves transient or recurrent discomfort triggered by mild stimuli, potentially accompanied by erythema [7].

While the biological mechanisms of general skin aging have been extensively investigated, the key mechanism and a holistic solution of sensitive skin aging remains underexplored. Recent comparative studies have highlighted distinct aging characteristics between sensitive and normal skin types [8, 9]. One emerging key master player in sensitive skin aging is CCN1

(Cellular Communication Network Factor 1, also known as CYR61), an extracellular matrix (ECM)-associated matricellular protein involved in barrier function, inflammatory signaling, collagen degradation, and cell-ECM communication [10-13]. CCN1 interacts with integrins on all skin cells and elevated CCN1 expression has been associated with impaired barrier function, fibroblast dysfunction, elevated pro-inflammatory cytokine levels, diminished collagen production, and ECM degradation. These combined effects disrupt the dermal ecosystem homeostasis in sensitive skin, ultimately accelerating the aging process [11, 14-16]. Therefore, targeting CCN1 may presents a novel approach to combat stress-induced aging and reshape sensitive skin ecology.

To investigate CCN1 as a therapeutic target for sensitive skin aging encology, we aim to develop a multi-stress aging in vitro model that mimics sensitive skin aging under real-world environmental challenges, including oxidative stress (H_2O_2), ultraviolet radiation, high glycation exposure, and high temperature exposure exposure etc. Given the broad complexity of these stressors, this study focuses on the oxidative stress (H_2O_2) model as the primary pathway of interest. high glycation exposure modle is briefly referenced to support prior findings, while UV and heat models are reserved for future investigation.

In a high-throughput screening guided by AI molecular docking, ashwagandha-a traditional adaptogenic herb known for stress resilience-was identified as a promising modulator of CCN1 signaling [17-20]. In this study, we evaluated the effects of ashwagandha root extract (ARE) on CCN1 expression and sensitive skin aging, using both in vitro fibroblast assays and a clinical trial. Our preliminary findings reveal a novel strategy targeting CCN1 to restore skin homeostasis, mitigate inflammation, and promote resilience against stress-induced aging in sensitive skin.

2. Materials and Methods

2.1 Materials

Ashwagandha root was purchased from Bozhou Guoxu Pharmaceutical Co., Ltd in 2024，lot number:24052201, Fibroblasts (HFF-1, Meisen), β-galactosidase staining kit (C0602, Beyotime), BCA protein assay kit (WB0123, Biotechwell), H_2O_2 (H112519-500, Aladdin), and CCK-8 (BN15201, Biorigin) were used. ELISA kits for CCN1 (M1591147), AP-1 (M1026490), COL1 (M1057630), MMP-1 (M1038199), ITGα2β1 (M1037342), ITGα6β1 (M1063737), and IL-16 (M1053097) were from Mlbio; IL-1β kit (L240418776) was from Cloud-Clone.

2.2 Methods

2.2.1 Preparation and Characterization of ashwagandha root extract

Ashwagandha root was extracted with an in-house patented method with water, filtered, and purified to obtain ARE. The content of Withanolide A was determined and optimized using an Agilent 1260 Infinity HPLC system equipped with a C18 column. The mobile phase consisted of water (A) and methanol (B), with a gradient elution as follows: 80% A / 20% B at 0 min, 0% A / 100% B at 6 min, maintained until 10 min. Other conditions were: column temperature 25 °C, injection volume 10 µL, flow rate 1 mL/min, and detection at 230 nm. Withanolide content was calculated based on a Withanolide A standard curve.

2.2.2 Oxidative Stress(H_2O_2)-Induced Aging Model in Fibroblasts

Human foreskin fibroblasts were cultured in DMEM with 15% FBS. Oxidative stress was induced by exposing cells to varying concentrations of H_2O_2 for 24 h. Cell viability was assessed using the CCK-8 assay, and senescence was evaluated by SA-β-gal staining. CCN1

protein levels were quantified by ELISA, with total protein normalized via BCA assay. Based on these results, the optimal H_2O_2 concentration for inducing senescence was selected to establish the cell aging model. To determine the safe and effective dose of ARE, fibroblasts were treated with graded concentrations of ARE, and cell viability was measured. Concentrations maintaining >80% viability were selected for downstream assays.

2.2.3 Protein Quantification by ELISA

Levels of CCN1, Activator Protein 1(AP-1), Integrinα2β1（ITGα2β1), Integrinα6β1(ITGα6β1), matrix metalloproteinase-1(MMP-1), COL1, interleukin-6(IL-6), and interleukin-1β（IL-1β) were measured using commercial ELISA kits, following manufacturers' instructions. All in vitro experiments were conducted in triplicate, and data are presented as mean ± standard deviation (SD). Statistical analysis was performed using GraphPad Prism 9.5. One-way or two-way analysis of variance (ANOVA) was used to determine statistical significance, with p-values interpreted as follows: $P < 0.05$ (*), $P < 0.01$ (**), $P < 0.001$ (****), and $P < 0.0001$ (****).

2.2.4 Clinical Evaluation of Sensitive Skin

A 28-day open-label study was conducted in over 30 Chinese women aged 20–55 years with clinically sensitive skin—defined by a questionnaire score ≥4 and a lactic acid sting test score ≥3 (as shown in Tables 1 and 2 for evaluation criteria)—and visible signs of facial aging. Clinical assessments were performed under standardized environmental conditions (21 ± 1 °C temperature and 50 ± 10% relative humidity). Imaging assessments (VISIA, PRIMOS-CR, Antera 3D, and VECTRA H2) and instrumental evaluations (Corneometer CM 825 for skin hydration and Cutometer dual MPA580 for elasticity and firmness) were conducted on Days 0, 7, and 28. Online self-evaluation questionnaires were completed on Days 14 and 21. Inferential statistics were performed using SPSS, with a two-tailed significance threshold of $\alpha = 0.05$. Paired t-tests were applied for instrumental measurements with normal distribution, while the Wilcoxon signed-rank test was used for non-normally distributed data. For binary outcome variables, binomial tests were performed under the assumption of a 50% agreement rate; statistical significance was defined as $P < 0.05$ with an observed agreement rate exceeding 50%.

Table 1. Subjective Sensitivity Questionnaire Scoring Criteria

Item	0	1	2	3
1.Discomfort (burning, redness, itching, stinging, tightness) during seasonal or temperature changes	Never	Occasionally	Frequently	Every time
2. Redness, itching, stinging, or tightness triggered by physical (e.g., exercise, collision) or emotional (e.g., stress) factors	Never	Occasionally	Frequently	Every time
4.Discomfort (burning, redness, itching, stinging, tightness) triggered by cosmetics or jewelry	Never	Occasionally	Frequently	Every time
5.Self-perceived skin sensitivity	Not sensitive	Mildly sensitive	Moderately sensitive	Very sensitive

Table 2. Lactic Acid Sting Test Scoring Criteria

Score	Description
0	No stinging sensation
1	Mild stinging
2	Moderate stinging, tolerable
3	Severe stinging, intolerable

3. Results

3.1 Characterization of ARE

As described, ARE was obtained via an in-house patented extraction method. Withanolide A was identified as the marker compound based on literature, and its presence was quantified and optimized by HPLC analysis.

3.2 In Vitro Cellular Experiment Results

3.2.1 Oxidative Stress(H_2O_2)-Induced Aging Model

A cellular model of oxidative stress-induced senescence was established using H_2O_2 in human dermal fibroblasts. As shown in Figure 1(a), cell viability decreased in a dose-dependent manner following 24-hour H_2O_2 exposure, with 0.21 mM reducing viability to 82.5%, a level suitable for modeling without inducing excessive cytotoxicity. At this concentration, CCN1 expression was significantly elevated as shown in Figure 1(b), and SA-β-gal staining revealed a marked increase in senescent cells compared to control in Figures 1(c). These findings indicate that treatment with 0.21 mM H_2O_2 for 24 hours effectively induces oxidative stress and senescence, accompanied by CCN1 upregulation, providing a robust model for subsequent investigations.

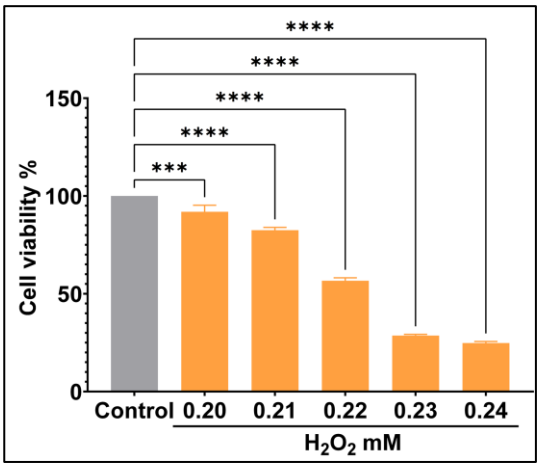

(**a**)

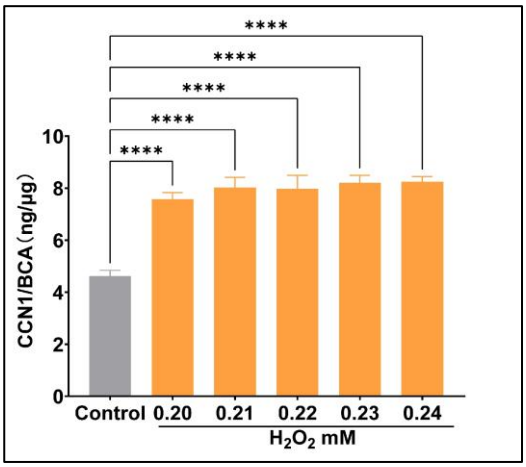

(**b**)

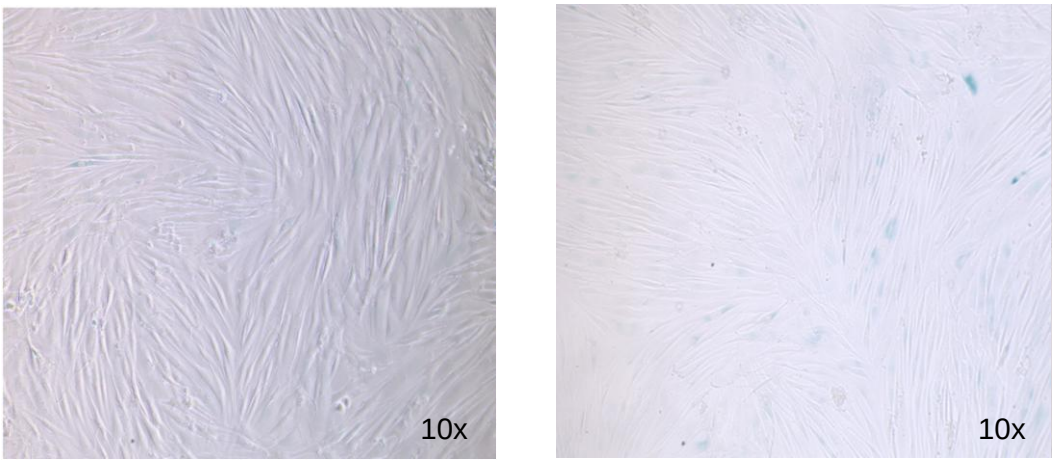

(**c1**) (**c2**)

Figure 1. Establishment of a oxidative stress(H_2O_2)-induced aging model model of H_2O_2-cultured fibroblasts with high expression of CCN1. (a) Cell viability of fibroblasts cultured with different concentrations of H_2O_2. (b) CCN1/BCA expression in fibroblasts cultured with different concentrations of H_2O_2. (c) SA-β-gal staining comparison to assess cellular senescence, (c1) Control cells; (c2) Cells treated with 0.21 mMH_2O_2.

3.2.2 ARE Concentration Screening

Fibroblasts were treated with various concentrations of ARE for 24 h. As shown in Figure 2(a), cell viability remained above 80% at concentrations ≤1.5%. However, 1.5% exhibited significant cytotoxicity compared to the control (****P < 0.0001), so 1.0%, 0.5%, and 0.1% were selected for further study. Under oxidative stress conditions, ARE at 1.0% and 0.5% significantly restored fibroblast viability compared to the model group (**P < 0.01), as shown in Figure 2(b). In contrast, 0.1% ARE showed no statistically significant difference from the model group (P > 0.05), indicating dose dependence as expected.

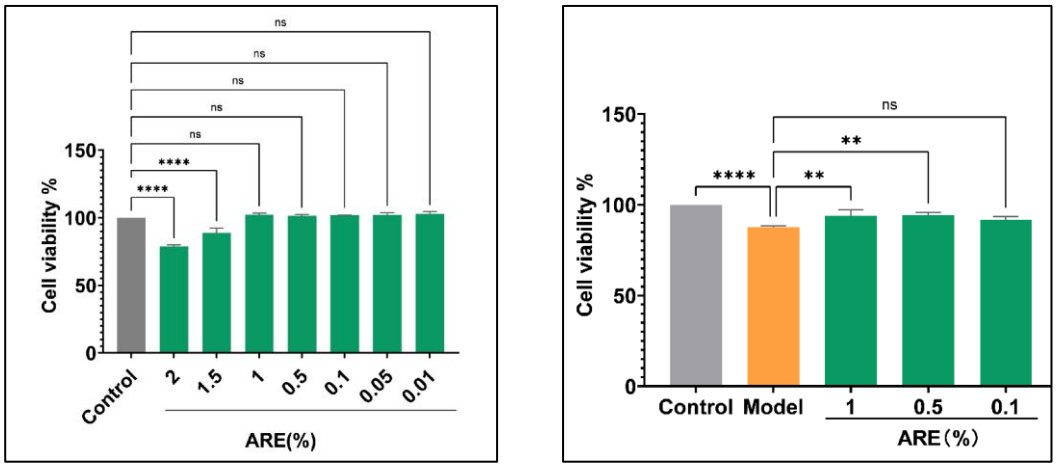

(**a**) (**b**)

Figure 2. Effects of ARE on cell viability in H_2O_2-induced aging model in fibroblasts. (a) Cytotoxicity assessment of ARE in fibroblasts after 24h treatment with different ARE concentrations. (b)Protective effects of ARE against H_2O_2-induced oxidative stress.

3.2.3 AP-1 and CCN1 Expression in Oxidative Stress(H_2O_2)-Induced Aging Model

As shown in Figure 3(a), ARE significantly reduced CCN1 expression in oxidative stress induced aging model in fibroblasts at all tested concentrations. A dose-dependent reduction in CCN1 levels was observed, with decreases of 50.85%, 27.17%, and 21.30% at high, medium, and low concentrations, respectively, compared to the model group. As shown in Figure 3(b), ARE treatment resulted in a statistically significant, dose-dependent reduction in AP-1 expression, with decreases of 28.40%, 14.47%, and 12.43% at high, medium, and low concentrations, respectively, relative to the model group (**P < 0.0001).

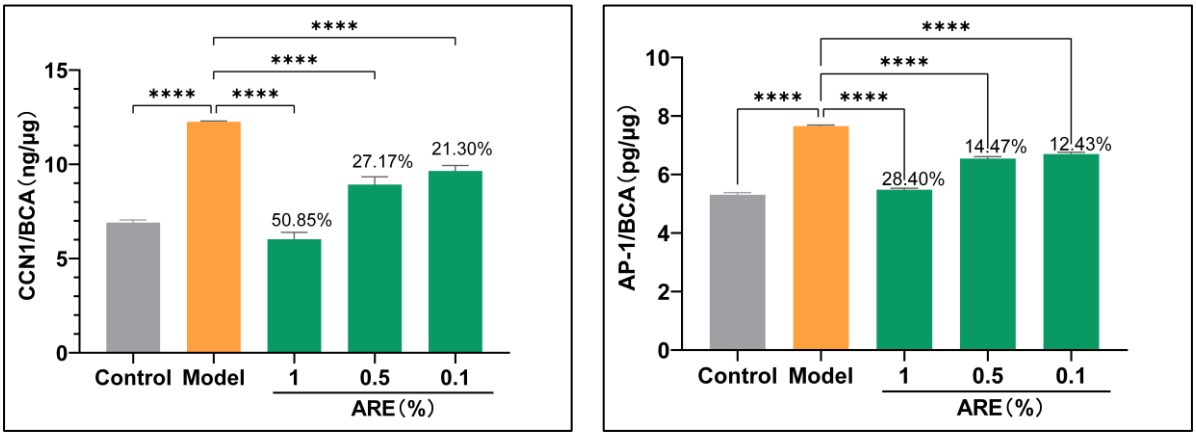

(**a**) (**b**)

Figure 3. ARE regulates CCN1 and AP-1 expression in oxidative stress(H_2O_2)-induced aging Model (a) Effects of different concentrations of ARE on CCN1 expression. (b) Effects of different concentrations of ARE on AP-1 expression

3.2.4 MMP-1 and COL-1 Expression in Oxidative Stress(H_2O_2)-Induced Aging Model

As shown in Figure 4(a), ARE significantly suppressed the upregulation of MMP-1 induced by H_2O_2 in a dose-dependent manner. Compared to the model group, the inhibition rates of MMP-1 expression were 39.65% (1.0%), 32.59% (0.5%), and 29.23% (0.1%), all showing significant differences (****P < 0.0001). As shown in Figure 4(b), ARE significantly reversed the H_2O_2-induced down regulation of collagen type I (COL-1) expression. ARE enhanced COL-1 levels by 18.58% (1.0%), 13.80% (0.5%), and 9.02% (0.1%) compared to the model group, with significant effects observed at all tested concentrations(****P < 0.0001 or ***P < 0.001).

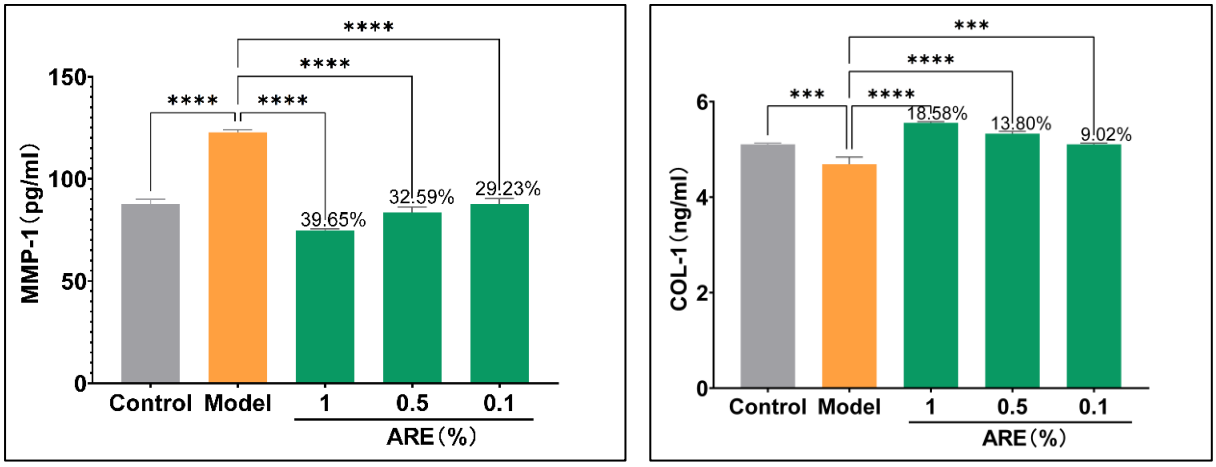

(**a**) (**b**)

Figure 4. ARE Regulates MMP-1 and COL-1 Expression in oxidative stress(H_2O_2)-induced aging model (a) Effects of different concentrations of ARE on MMP-1 expression. (b) Effects of different concentrations of ARE on COL-1 expression.

3.2.5 Integrin Expression in Oxidative Stress(H_2O_2)-Induced Aging Model

As shown in Figure 5(a), ARE significantly upregulated ITGα2β1 expression in a dose-dependent manner. Compared with the model group, ITGα2β1 expression increased by 78.80% (1.0%), 65.07% (0.5%), and 54.35% (0.1%), all showing significant differences (**P < 0.01 or ***P < 0.001). Conversely, Figure 5(b) shows that ARE significantly suppressed the overexpression of ITGα6β1 induced by H_2O_2. The inhibition rates were 48.97% (1.0%), 16.16% (0.5%), and 7.94% (0.1%), with significant reductions observed at all concentrations. (**P < 0.01 or ****P < 0.0001).

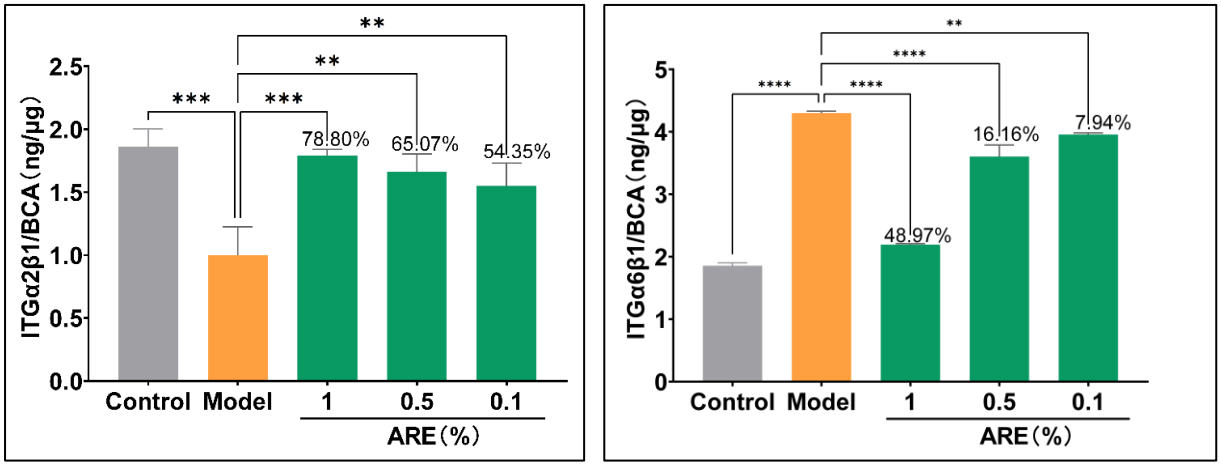

(**a**) (**b**)

Figure 5. ARE Regulates Integrin Expression in oxidative stress(H_2O_2)-induced aging model. (a) Effects of different concentrations of ARE on ITGα2β1 expression. (b) Effects of different concentrations of ARE on ITGα6β1 expression)

3.2.6 Pro-inflammatory Cytokine Expression in Oxidative Stress(H_2O_2)-Induced Aging Model

As shown in Figure 6(a), ARE significantly reduced the overexpression of IL-1β by H_2O_2 in a dose-dependent manner. Compared with the model group, ARE suppressed IL-1β expression by 48.03% (1.0%), 45.17% (0.5%), and 41.24% (0.1%) (****P < 0.0001). Similarly, Figure 6(b) shows that ARE markedly downregulated IL-6 levels. The inhibition rates were 25.44% (1.0%), 24.21% (0.5%), and 23.93% (0.1%), all significantly different from the model group (****P < 0.0001).

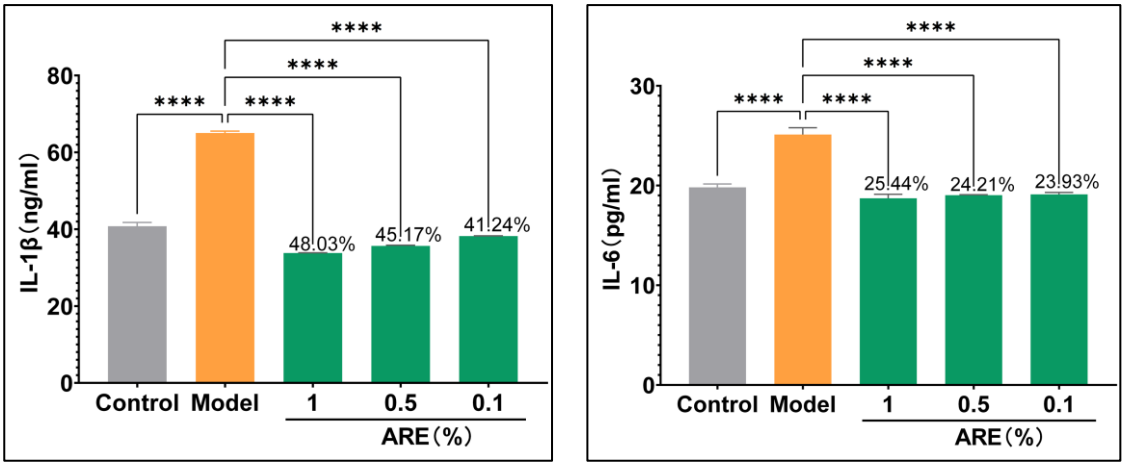

(**a**) (**b**)

Figure 6. ARE Attenuates Pro-inflammatory Cytokine Expression in oxidative stress(H_2O_2)-induced aging model. (a) Effects of different concentrations of ARE on IL-1β expression. (b) Effects of different concentrations of ARE on IL-6 expression.

3.3 Clinical Trial Results

A 28-day clinical trial was conducted on 31 volunteers with sensitive skin (lactic acid stinging score ⩾ 3) to evaluate the efficacy and safety of a model topical cream containing with 1.8% of ARE.

3.3.1 Clinical Safety Assessment in Sensitive Skin Subjects

After 28 days of continuous application of the ARE-containing cream by 31 subjects with sensitive skin (lactic acid stinging score⩾3), no adverse skin reactions were observed, indicating good safety for sensitive skin.

3.3.2 Skin Hydration, Elasticity, and Firmness

As shown in Figure 7, significant improvements were observed in key skin parameters compared to baseline (D0). Stratum corneum hydration increased by 48.96%, skin elasticity (Q1) improved by 27.20%, and skin firmness (F4) was reduced by 32.40%, reflecting enhanced skin hydration, elasticity, and firmness, respectively (***P < 0.001 for all).Note: Higher values of hydration and Q1indicate better moisture and elasticity, respectively, while lower F4 values reflect improved firmness.

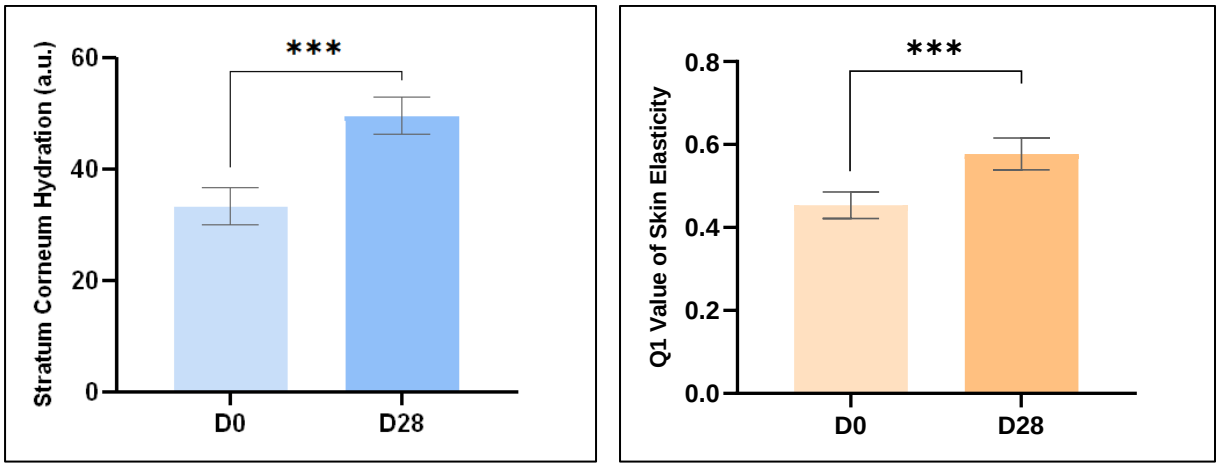

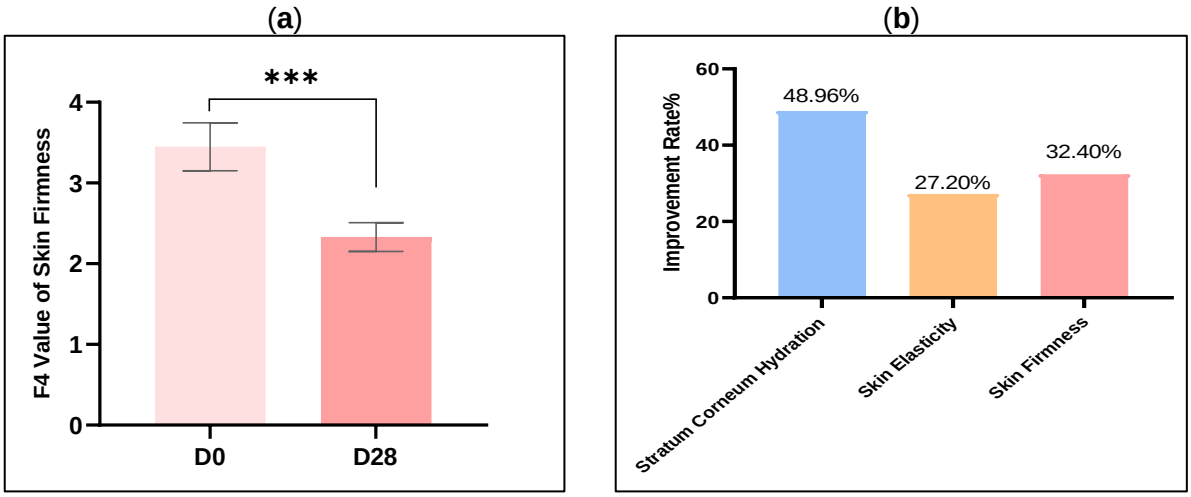

Figure 7. Improvements in skin hydration, elasticity, and firmness. (a)Stratum corneum hydration levels at baseline (D0) and Day 28, (b)kin elasticity (Q1 values) at baseline and Day 28, (c)Skin firmness (F4 values) at baseline and Day 28, (d)Percent improvement rates of all three parameters after 28 days of treatment.)

3.3.3 Nasolabial Folds(NLFS)

As shown in Figure 8, ARE-containing cream demonstrated visible anti-aging efficacy on NLFS. The radar chart in Figure 8(a) illustrates significant improvements across five clinical parameters after 28 days. Specifically, the number of NLFS was reduced by 33.33%, wrinkle length by 16.94%, average width by 11.56%, average depth by 14.92%, and surface roughness (Ra value) by 29.15%. These results indicate comprehensive improvements in wrinkle severity and texture. In addition, representative clinical images as in Figure 8(b) taken on Day 0, Day 7, and Day 28 show a visible reduction in the appearance of NLFS over time, supporting the quantitative findings.

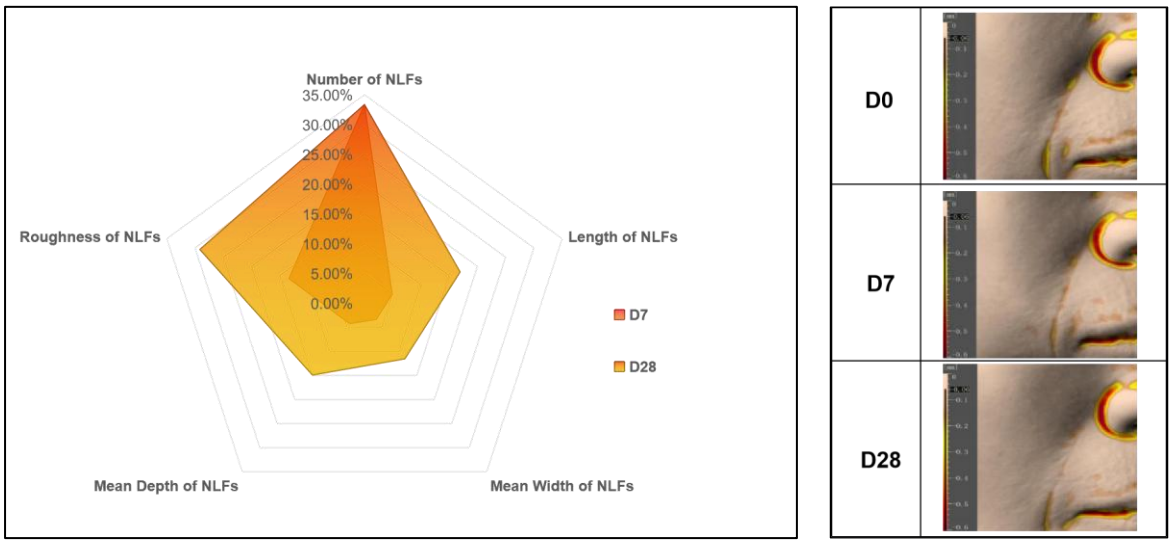

Figure 8. Clinical efficacy of ARE cream on NLFS after 28 days of application.(a)Radar chart showing percent improvement in five wrinkle parameters: number, length, average width, average depth, and surface roughness (Ra), (b) Representative clinical photographs of na-

solabial folds taken at Day 0, Day 7, and Day 28.Visible reductions in wrinkle severity and texture were observed, consistent with quantitative measurements.

3.3.4 Crow's Feet Wrinkles(CFW)

As shown in Figure 9, ARE-containing cream demonstrated visible anti-aging efficacy on CFW. The radar chart in Figure 9(a) illustrates significant improvements across five clinical parameters after 28 days. Specifically, the number of CFW was reduced by 25.93%, wrinkle area by 27.20%, mean length by 25.45%, Mean Depth by 20.97%, and surface roughness (Rz value) by 15.23%. These results indicate comprehensive improvements in wrinkle severity and texture. In addition, representative clinical images in Figure 9(b) taken on Day 0, Day 7, and Day 28 show a visible reduction in the appearance of CFW over time, supporting the quantitative findings.

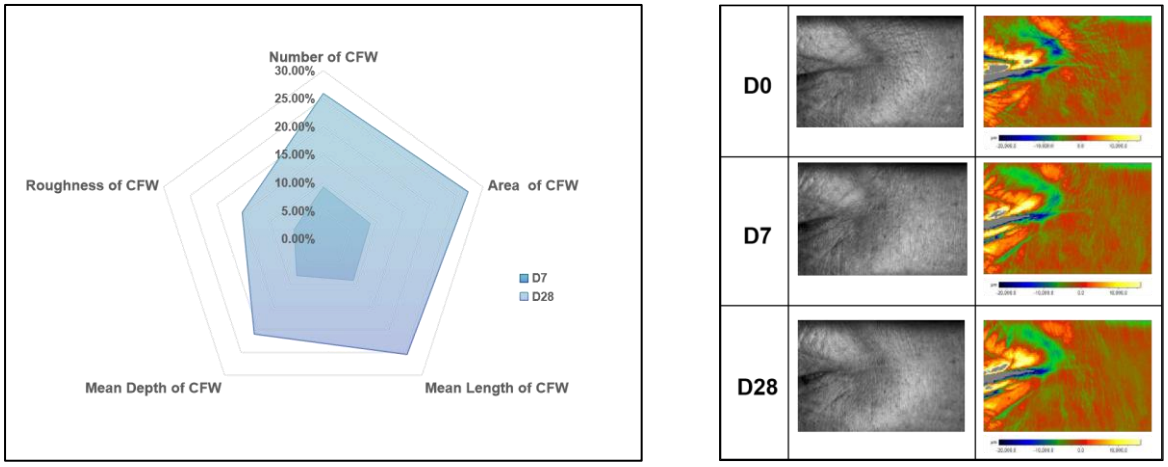

(**a**) (**b**)

Figure 9. Clinical efficacy of ARE cream on CFW after 28 days of application. (a)Radar chart showing percent improvement in five wrinkle parameters: number, area, mean length, mean depth, and surface roughness (Rz).(b) Representative clinical photographs of crow's feet taken at Day 0, Day 7, and Day 28. Quantitative and visual data collectively demonstrate ARE's anti-wrinkle efficacy in the CFW region.

3.3.5 Infraorbital Wrinkles (IOW)

As shown in Figure 10, ARE-containing cream demonstrated visible anti-aging efficacy on IOW. The radar chart in Figure 10(a) illustrates significant improvements across five clinical parameters after 28 days. Specifically, the number of IOW was reduced by 33.33%, area by 26.18%, length by 16.94%, depth by 14.92%, and surface roughness (Ra value) by 29.15%. These results indicate comprehensive improvements in wrinkle severity and texture. In addition, representative clinical images in Figure 8(b) taken on Day 0, Day 7, and Day 28 show a visible reduction in the appearance of IOW folds over time, supporting the quantitative findings.

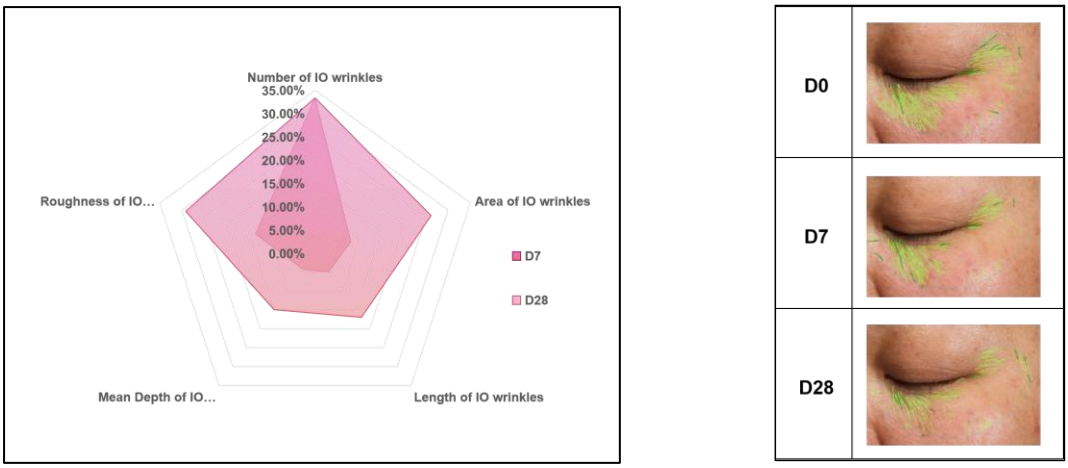

(**a**) (**b**)

Figure 10. Clinical efficacy of ARE cream on IOW after 28 days of application.(a)Radar chart showing percent improvement in five wrinkle parameters: number, area, mean length, mean depth, and surface roughness (Rz).(b) Representative clinical photographs of IOW taken at Day 0, Day 7, and Day 28. Quantitative and visual data collectively demonstrate ARE's anti-wrinkle efficacy in the IOW region.

3.3.6 Facial Contour

As shown in Figure11, significant improvements were observed in key skin parameters compared to baseline (D0). Jawline Length reduced by 1.96%, Jaw Angle reduced by 1.56 %, and Apple Zone Volume was reduced by 5.68%, reflecting enhanced facial contour, respectively (***P < 0.001 for all). Note: Lower values of Jawline Length and Jaw Angle indicate better facial contour, respectively, while higher Apple Zone Volume reflect improved facial contour.

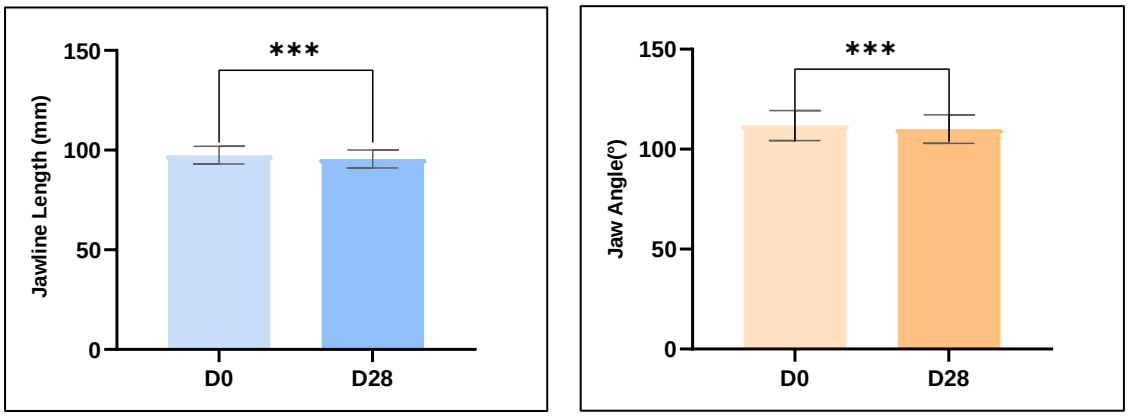

(**a**) (**b**)

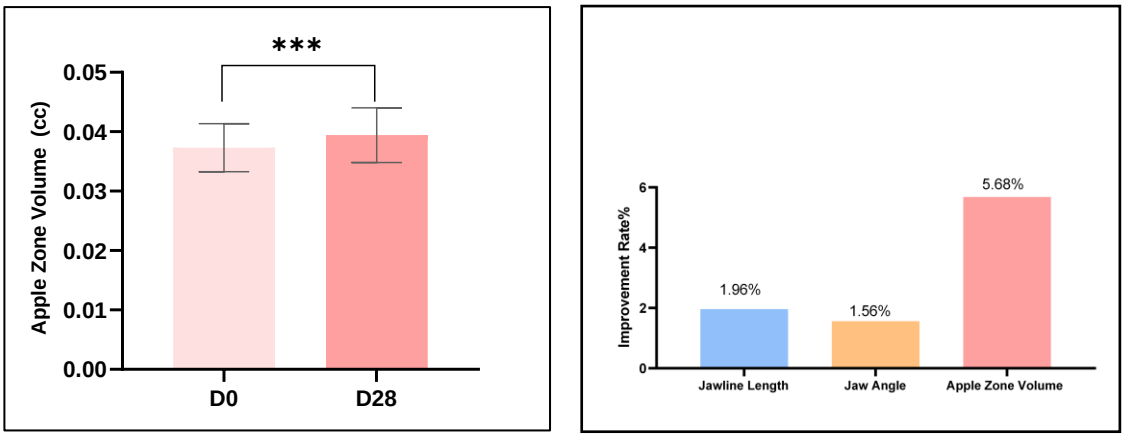

(**c**) (**d**)

Figure 11. Clinical efficacy of ARE cream on Facial Contour after 28 days of application.(a–c)Changes in Jawline Length, Jaw Angle , and Apple Zone Volume from Day 0 to Day 28.(d)Percent improvement in all parameters at Day 28 vs. basline).

4. Discussion

4.1 Role of CCN1 in Skin Aging and Sensitivity Regulation

CCN1, a matricellular protein, plays a pivotal role in the regulation of inflammation, ECM remodeling, and integrin-mediated signaling—all of which are central to the pathogenesis of skin aging and sensitivity. As a key component of the senescence-associated secretory phenotype (SASP), CCN1 is upregulated in response to oxidative stress and contributes to the expression of pro-inflammatory cytokines and MMPs, leading to barrier dysfunction, collagen degradation and dermal structure disruption.

In the present study, a model oxidative stress induced by H_2O_2 significantly elevated CCN1 expression in human dermal fibroblasts, confirming its role in redox-sensitive skin aging pathways. Treatment with ARE resulted in a marked downregulation of CCN1, alongside suppression of IL-1β, IL-6 and MMP-1, and upregulation of COL I, suggesting that ARE mitigates sensitive skin aging by rebalancing ECM degradation and synthesis. Furthermore, ARE modulated integrin signaling by increasing ITGα2β1 expression and decreasing ITGα6β1, indicating enhanced cell–matrix adhesion and improved mechanotransduction. This remodeling of integrin profiles is likely to contribute to improved skin elasticity and barrier homeostasis. Together, these findings establish CCN1 as a central regulator of sensitive skin aging and underscore ARE's therapeutic potential in targeting CCN1 related sensitive skin aging.

4.2 Clinical Significance and Limitations of Human Trial

The clinical results demonstrated that ARE-containing cream significantly improved multiple aspects of skin health, including hydration (+48.96%), elasticity (+27.2%), and firmness (+32.4%) after 28 days of use. In addition, a comprehensive improvement in wrinkle-related parameters—such as number, length, depth, and roughness-was observed in both crow's feet and nasolabial folds. These findings provide translational evidence supporting the in vitro results and validate ARE's efficacy in real-world application. Importantly, the trial was conducted on sensitive skin subjects and showed excellent tolerability with no adverse skin reactions reported, highlighting the extract's suitability for this demanding skin type. The dual

function of ARE-targeting both sensitivity and aging-addresses a current unmet need in dermocosmetics.

Nevertheless, limitations of this study should be acknowledged. The sample size (n=31) was relatively small, and the study duration (28 days) may not fully capture the long-term benefits or biological remodeling associated with anti-aging interventions. Quantitative assessment of facial contour improvement was partially limited to photographic evidence. Future trials with larger cohorts, longer follow-up, and the inclusion of high-resolution biophysical and -omics-based assessments are warranted to validate and extend the current findings.

4.3 Sensitive Skin Multi-Stress Aging Models

As mentioned, we aim to develop a sensitive skin multi-stress aging model incorporating H_2O_2, UV, high glucose (MGO), and heat to mimic real-world stressors. Besides the detail dicussion on H_2O_2-induced stress model in this study, in our previous study using an MGO-induced glycation stress agine model [21], ARE also significantly ameliorated MGO-induced skin barrier damage by restoring key structural proteins such as fibronectin I, laminin 5, and tenascin C. ARE also upregulated ITGB1 expression, reduced the levels of MMP-2 and MMP-9, and improved aging-related markers such as COL1 and TGF-β1. MGO-induced high-glycation environments are well known to trigger pronounced cellular senescence. Meanwhile, elevated CCN1 expression is a recognized hallmark of aged skin. Therefore, we hypothesize that ARE may exert its protective effects against glycation-induced aging, at least in part, by modulating CCN1 expression. This is further supported by evidence showing that advanced glycation end-products (AGEs), such as CML, induce low-grade chronic inflammation and extracellular matrix degradation—features commonly associated with CCN1 upregulation. Taken together, these findings suggest that CCN1 could be a potential target through which ARE mitigates glycation-driven skin aging, and future studies directly examining CCN1 expression in MGO models will be essential to validate this hypothesis. Similarly other stress-induced age model including UV and heat will also be explored.

As demonstrated in Figure 12, by effectively targeting the master key, CCN1, which interacts with integrins on all types of skin cells, triggering inflammation, barrier dysfunction, collagen loss, and ECM degradation, ARE shows the potential of reshaping sensitive skin ecology and combating multi-stress-induced aging.

5. Conclusion

This study provides compelling evidence that ARE exerts multifaceted protective effects against skin aging and sensitivity. In an H_2O_2-induced oxidative stress model, ARE significantly downregulated the expression of CCN1, a critical mediator of inflammatory and extracellular matrix-degrading processes, while restoring collagen synthesis and modulating integrin signaling. These molecular changes translated into improved cellular resilience and dermal structural integrity, underscoring the relevance of CCN1 as a novel therapeutic target for sensitive skin aging. Complementary in vivo findings from a randomized, controlled clinical trial demonstrated that 28-day topical application of ARE-containing cream led to significant improvements in skin hydration, elasticity, firmness, and a visible reduction in wrinkle severity across multiple facial regions. The favorable outcomes in a population with sensitive skin further highlight the extract's safety and suitability for vulnerable skin types. Moreover, data from an independent MGO-induced glycation model, though not directly linked to CCN1 modulation, confirmed ARE’s anti-senescence activity under a different aging stressor, reinforcing its broad-spectrum efficacy.

To our knowledge, this is the first study to integrate CCN1 signaling, multi-stress model mechanistic exploration, and clinical validation to establish Ashwagandha as a promising active ingredient for sensitive skin anti-aging care. CCN1's role also extends beyond skin, with oral studies suggesting potential gut health benefits. These findings pave the way for future formulation development and provide a scientific basis for ARE's incorporation into dermatological and intake oral applications aimed at holistic beauty and overall wellness.

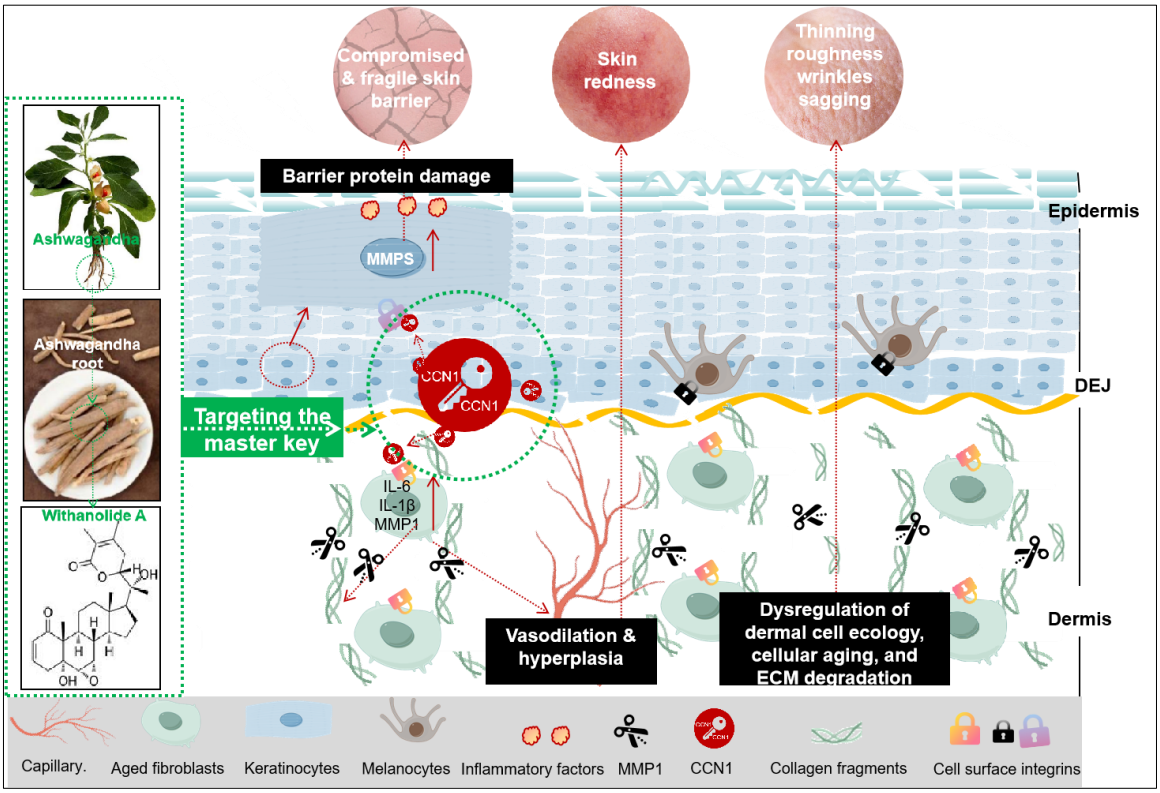

Figure 12. Mechanism of Ashwagandha Targeting CCN1 for Skin Health and Beauty

Reference

[1] E.T. Bernstein, Cleansing of Sensitive Skin, Journal of Investigative Dermatology 9(1) (1947) 5-9.

[2] L. Misery, S. Stander, J.C. Szepietowski, etal, Definition of Sensitive Skin: An Expert Position Paper from the Special Interest Group on Sensitive Skin of the International Forum for the Study of Itch, Acta Derm Venereol 97(1) (2017) 4-6.

[3] C. J, C. G, J. Y, etal, Sensitive skin syndrome: Research progress on mechanisms and applications, Journal of Dermatologic Science and Cosmetic Technology 1(2) (2024).

[4] L. Misery, K. Loser, S. Stander, Sensitive skin, J Eur Acad Dermatol Venereol 30 Suppl 1 (2016) 2-8.

[5] A. Wollenberg, A. Gimenez-Arnau, Sensitive skin: A relevant syndrome, be aware, J Eur Acad Dermatol Venereol 36 Suppl 5 (2022) 3-5.

[6] L. H, J. Z, H. M, etal, Chinese expert consensus on the diagnosis and treatment of sensitive skin. , Chinese Journal of Dermatovenereology 31(1) (2017) 4.

[7] L. H, Guidelines for the Diagnosis and Treatment of Sensitive Skin in China(2024 Edition), The Chinese Journal of Dermatovenereology 38(5) (2024) 8.

[8] F. Y, X. K, G. L, etal, The Chinese female facial skin database construction and utilization Deciphering the Ageing status of Chinese sensitive females, 33rd IFSCC Congress (2023).
[9] X. K, F. Y, X. Y, etal, A study on the differences between sensitive skin and normal skin in the mechanisms and patterns of skin aging based on skin status ，database Detergent & Cosmetics 47(3) (2024) 43-54+60.
[10] K. Grote, G. Salguero, M. Ballmaier, etal, The angiogenic factor CCN1 promotes adhesion and migration of circulating CD34+ progenitor cells: potential role in angiogenesis and endothelial regeneration, Blood 110(3) (2007) 877-85.
[11] Y. Sun, J. Zhang, Z. Zhou, etal, CCN1, a Pro-Inflammatory Factor, Aggravates Psoriasis Skin Lesions by Promoting Keratinocyte Activation, J Invest Dermatol 135(11) (2015) 2666-2675.
[12] Z. Xu, L. Chen, M. Jiang, etal, CCN1/Cyr61 Stimulates Melanogenesis through Integrin alpha6beta1, p38 MAPK, and ERK1/2 Signaling Pathways in Human Epidermal Melanocytes, J Invest Dermatol 138(8) (2018) 1825-1833.
[13] T. Quan, T. He, Y. Shao, etal, Elevated cysteine-rich 61 mediates aberrant collagen homeostasis in chronologically aged and photoaged human skin, Am J Pathol 169(2) (2006) 482-90.
[14] T. Quan, S. Shin, Z. Qin, etal, Expression of CCN family of genes in human skin in vivo and alterations by solar-simulated ultraviolet irradiation, J Cell Commun Signal 3(1) (2009) 19-23.
[15] T. Quan, Z. Qin, P. Robichaud, etal, CCN1 contributes to skin connective tissue aging by inducing age-associated secretory phenotype in human skin dermal fibroblasts, J Cell Commun Signal 5(3) (2011) 201-7.
[16] Y. Sun, J. Zhang, T. Zhai, etal, CCN1 promotes IL-1beta production in keratinocytes by activating p38 MAPK signaling in psoriasis, Sci Rep 7 (2017) 43310.
[17] S. Lee, Y.J. Choi, S. Lee, etal, Protective Effects of Withagenin A Diglucoside from Indian Ginseng (Withania somnifera) against Human Dermal Fibroblast Damaged by TNF-alpha Stimulation, Antioxidants (Basel) 11(11) (2022).
[18] P.V. Babu, A. Gokulakrishnan, R. Dhandayuthabani, etal, Protective effect of Withania somnifera (Solanaceae) on collagen glycation and cross-linking, Comp Biochem Physiol B Biochem Mol Biol 147(2) (2007) 308-13.
[19] S.K. Meher, B. Das, P. Panda, etal, Uses ofWithania somnifera(Linn) Dunal (Ashwagandha) in Ayurveda and its Pharmacological Evidences, Research Journal of Pharmacology and Pharmacodynamics 8(1) (2016).
[20] J. Nass, S. Abdelfatah, T. Efferth, Induction of stress resistance and extension of lifespan in Chaenorhabditis elegans serotonin-receptor knockout strains by withanolide A, Phytomedicine 84 (2021) 153482.
[21] X. Liu, C. Chen, Y.e.a. Lin, Withania somnifera root extract inhibits MGO-induced skin fibroblast cells dysfunction via ECM-integrin interaction, J Ethnopharmacol 323 (2024) 117699.